

Exploring the channel connectivity structure of the August 2008 avulsion belt of the Kosi River, India: Application to flood risk assessment

R. Sinha¹, K. Gaurav¹, S. Chandra¹, and S.K. Tandon²

¹Department of Civil Engineering, Indian Institute of Technology, Kanpur 208016, India

²Shiv Nadar University, Greater Noida, UP, India, and Indian Institute of Technology, Kanpur 208016, India

ABSTRACT

The August 2008 avulsion of the Kosi River, northern India, resulted in a maximum eastward shift of >100 km and created an avulsion belt of 2722 km². Based on A.D. 2000 Shuttle Radar Topography Mission data and on 2005 Landsat Thematic Mapper satellite image-derived channel network (pre-avulsion), we use a topography-driven connectivity model to simulate the avulsion pathway, which corresponds, to a large extent, to that observed in the post-avulsion period. We then use this model to postulate the avulsive course of the river from another upstream point based on avulsion threshold analysis. Our results demonstrate that this model has the potential for postulating the path of an avulsive channel, and can provide a priori information on the areas likely to be flooded following an embankment breach.

INTRODUCTION

The Kosi River is one of the important drainages of the Ganga basin (northern India; Fig. 1), with well-documented dominantly westward avulsive shifts aggregating >113 km across the fan surface over the past 200 yr (Gole and Chitale, 1966; Chakraborty et al., 2010). The Kosi has been jacketed since 1955–1956 by embankments on both the eastern (144 km long) and western (123.2 km long) sides; the distance between the two embankments varies from 4.8 to 16 km (Desai, 1982). In August 2008, a major breach of the eastern embankment at Kusaha (Nepal), 12 km upstream of the Kosi barrage, took place and resulted in an eastward avulsive shift of the river by >100 km at its maximum near Purnea, India (Sinha, 2009) (Fig. 1). The breach was plugged in January 2009, and the river was once again confined within the embankments.

The August 2008 avulsion was the first major eastward shift of the river during the post-embankment period (1955–1956) and 80%–85% of the total flow entered into the new course. The 1500-m-wide breach resulted in a sheet of water 15–20 km wide and 150 km long with a velocity of 1 m/s in the avulsion belt (United Nations Institute for Training and Research, 2008). This avulsion created an extensive inundation zone measuring 2722 km² that caused the waters of the Kosi River to reconnect to the paleochannel network on the fan surface. The August 2008 avulsion through the breach of the eastern embankment occurred at a peak flow of ~4078 m³/s, far lower than the design capacity of ~26,901 m³/s for the barrage downstream (Mishra, 2008). Field observations (Sinha, 2009) also indicated that the elevation of the Kosi river bed around Kusaha was ~4 m higher than that of the adjoining floodplain, and this accords well with earlier observations (cf. Desai, 1982) that concluded that aggradation of 2.44 m of the bed with respect to the 1984 level could occur within the embankments by 2005.

PRESENT STUDY AND APPROACH

This study explores the way in which the hydrological flux (river flow and groundwater seepage) was connected to the fan surface in the newly formed avulsion belt east of the breached embankment. Prior to the avulsion event, this terrain mostly consisted of small seepage channels, proximal to the embankment, and abandoned channels and/or paleochannels away from it. The terrain included a major paleochannel that was active ~100 yr ago (Gole and Chitale, 1966) and that acted as the main pathway for the avulsed waters in August 2008 (Fig. 1).

Our study has been designed to capture the topography-driven channel connectivity from Kusaha downstream into the avulsion belt (inundation zone) based on 2000 Shuttle Radar Topography Mission (SRTM) data (see the GSA Data Repository¹), and to compare this with the pre-avulsion and post-avulsion channel network connectivity based on Landsat Thematic Mapper (TM) satellite imagery. The study window was chosen from the avulsion point at Kusaha to the intersection of the avulsion channel, with a canal beyond which the channel network also became unconfined. The combined use of the digital elevation model (DEM) and the multitemporal satellite imagery data enables the detection of temporal changes in the channel network connectivity of any given terrain. The key question in this study is to test whether adequate connectivity information is embedded in the DEM to forecast major flow paths and the approximate extent of the inundation belt. The August 2008 avulsion provided such an opportunity for testing the match (or mismatch) between the topographically driven channel connectivity structure derived from the 2000 SRTM data and the newly formed avulsion belt.

Depending on the proportion of water and moisture content in the stream network, we have identified four classes of connectivity structures using the Landsat imagery (cf. Jain and Tandon, 2010): (I) inactive connected, (II) disconnected, (III) active connected, and (IV) partially

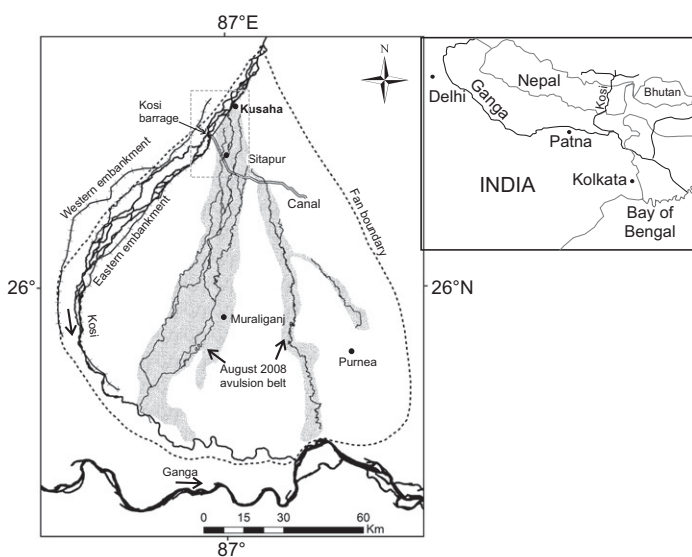


Figure 1. Map of Kosi megafan (northern India) showing area of August 2008 inundation (shaded) avulsion; dashed box represents modeled area for this study. Modern Kosi River flows along western margin of megafan measuring 155 × 115 km.

¹GSA Data Repository item 2013305, methods for image processing and SRTM data analysis, node selection and modeling algorithm, and field photographs showing major changes in connectivity structure, is available online at www.geosociety.org/pubs/ft2013.htm, or on request from editing@geosociety.org or Documents Secretary, GSA, P.O. Box 9140, Boulder, CO 80301, USA.

connected (Fig. 2). Class I represents an example of dry paleochannel with full structural connectivity (Wainwright et al., 2011) but with no functional connectivity, whereas class III represents an active channel with full structural and functional connectivity (Bracken and Croke; 2007; Wainwright et al., 2011). Similarly, class II represents an isolated channel with partial structural connectivity, and class IV represents a paleochannel with a few wet segments (full structural but partial functional connectivity).

DATA USED AND METHODOLOGY

We used the Landsat TM imagery of 05 November 2005 (pre-2008 avulsion) and 29 September 2009 (post-2008 avulsion) to map the temporal variability in different connectivity classes. The moderate spatial resolution (30 m) of Landsat images restricted the direct mapping of the channel network, but its wide spectral sensitivity in visible, infrared, and thermal infrared ranges were useful in identifying the paleochannels through moisture and water content on the post-monsoon satellite imageries (see the Data Repository). The combination of spectral band 4 (0.76–0.90 μm), band 5 (1.55–1.75 μm), and band 7 (2.08–2.35 μm) was used for generating the false color composite (FCC) (Fig. 3). A normalized difference water index (NDWI) was calculated, as it helps to delineate the surface-water features more accurately (McFeeters, 1996). On the basis of NDWI results, the connectivity of the streams was identified as connected, partially connected, and disconnected. After manually extracting the paleochannel network for the study window from the Landsat FCC as arcs, the stream junctions and bends were represented as nodes.

To quantify the change in the connectivity structure through time (pre-avulsion to post-avulsion), a change detection analysis was performed to assess the change in the connectivity of channel networks. The study area was divided into $200 \times 200 \text{ m}^2$ grids, and each grid was assigned a connectivity class. Also, a grid-wise change detection matrix between 2005 and 2009 was generated to quantify the amount of relative change in connectivity classes in each grid (Table 1).

We propose a connectivity index, I_c , to quantify the connectivity structure, as follows:

$$I_c = \frac{S_t}{L_t} \sum_{\text{dry channels}} \frac{L_d}{S_d}, \quad (1)$$

where L_d is the length of dry channels, S_d is the slope of dry channels, L_t is the total length, and S_t is the total slope between the start and end points. S_d was calculated based on the initial and final points of the particular dry channel, and the length of the channel (further illustration in Fig. DR1 in the Data Repository).

Higher values of I_c represent increasing disconnectivity, and $I_c = 0$ represents no dry channels (or a completely connected river).

We can define the percentage connectivity as $C\% = 100/(1 + I_c)$, which leads to an index ranging from 0 to 100; i.e., $C\% \in (0, 100]$ with $C\% = 100\%$ implying a fully connected river.

A semiautomated model (see Fig. DR2 for the flow chart) that helps to predict the most possible connected pathway of the stream in case of any flood event has been developed. The model uses the start, end, and junction nodes from the stream network manually extracted from Landsat FCC, and their corresponding elevation value from SRTM data. The program starts from a given point, and the algorithm models the best possible flow path of the stream using slope and relative proximity of the nodes based on a few assumptions.

1. The stream will never go from a node at a lower elevation to one at a higher elevation.
2. The stream will go on developing until it has reached the end of the map, or it has reached a global minimum.
3. If there are many valid nodes near the initial node, the path of the stream is decided by the slope, not the distance.
4. If no valid nodes appear within a fixed radius, the path is determined by the closest valid point.

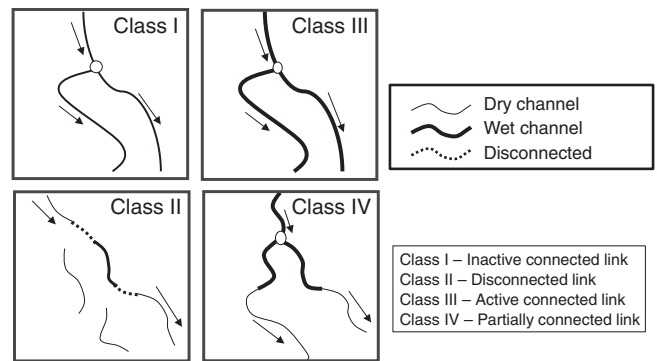


Figure 2. Schematic representation of different types of connectivity.

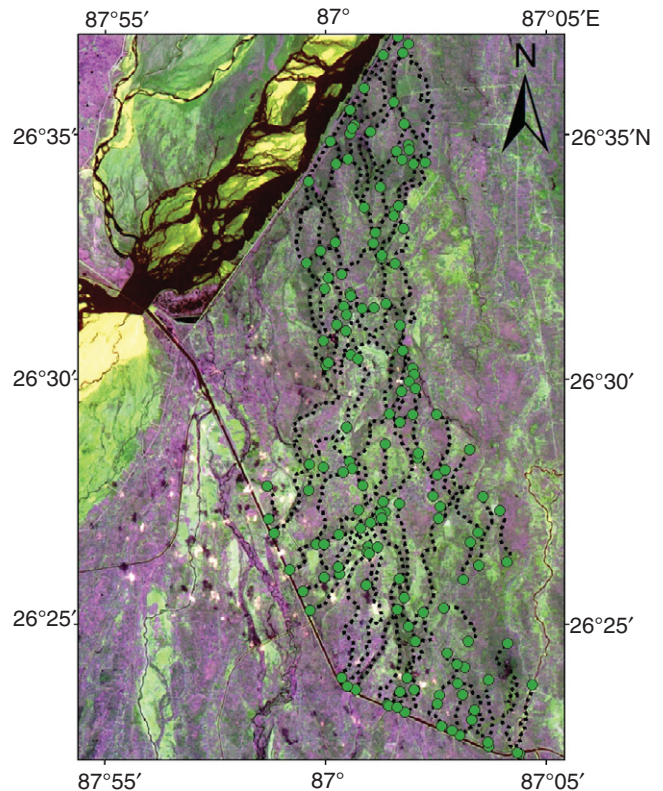


Figure 3. Landsat false color composite from 2 November 2005, from which paleochannel network (dashed lines) was extracted; stream junctions and bends are represented as nodes (green dots).

RESULTS AND DISCUSSION

Percent changes in the frequency of the streams in each connectivity class were calculated by taking the 2005 stream connectivity map as a baseline (Table 1). Figure 4 shows the grid ($200 \times 200 \text{ m}$) representation of different connectivity classes for 2005 and 2009. For purposes of calculation, the grids with no stream link have been considered as “no connectivity” class grids. Change detection analysis (Fig. 4, inset) shows that there is an increase in the number of active connected links (class III) between 2005 and 2009, whereas all other classes show significant decrease. This suggests that the functional connectivity of the system increased after the hydrological flux was connected to the avulsion belt. This is further validated from the field observation that the main avulsion channel, which was seasonal in the pre-avulsion period, now flows for most parts of the year (see Fig. DR3A). An interesting observation is a sizable increase in the “no connectivity” class at the expense of classes II and IV, caused by the filling of several abandoned channels on the fan surface (see

TABLE 1. CHANGE DETECTION MATRIX OF CHANNEL CONNECTIVITY STRUCTURE BETWEEN 2005 AND 2009

Connectivity class	No connectivity (2005)	I (2005)	II (2005)	III (2005)	IV (2005)	Class total in 2009
No connectivity (2009)	1696	26	634	1	230	2587
I (2009)	0	0	15	0	3	18
II (2009)	392	4	278	6	48	724
III (2009)	111	10	37	11	62	220
IV (2009)	34	0	8	0	76	118
Class total in 2005	2233	40	972	18	419	3682
Total change (% change)	+354 (+16%)	-22 (-55%)	-248 (-26%)	+202 (+1122%)	-301 (-72%)	

Note: Rows show the number of grids that changed from one class to another between 2005 and 2009. The row "class total in 2005" shows the number of grids for each class in 2005 and the column "class total in 2009" shows the same for 2009. The last row shows the total change between 2005 and 2009.

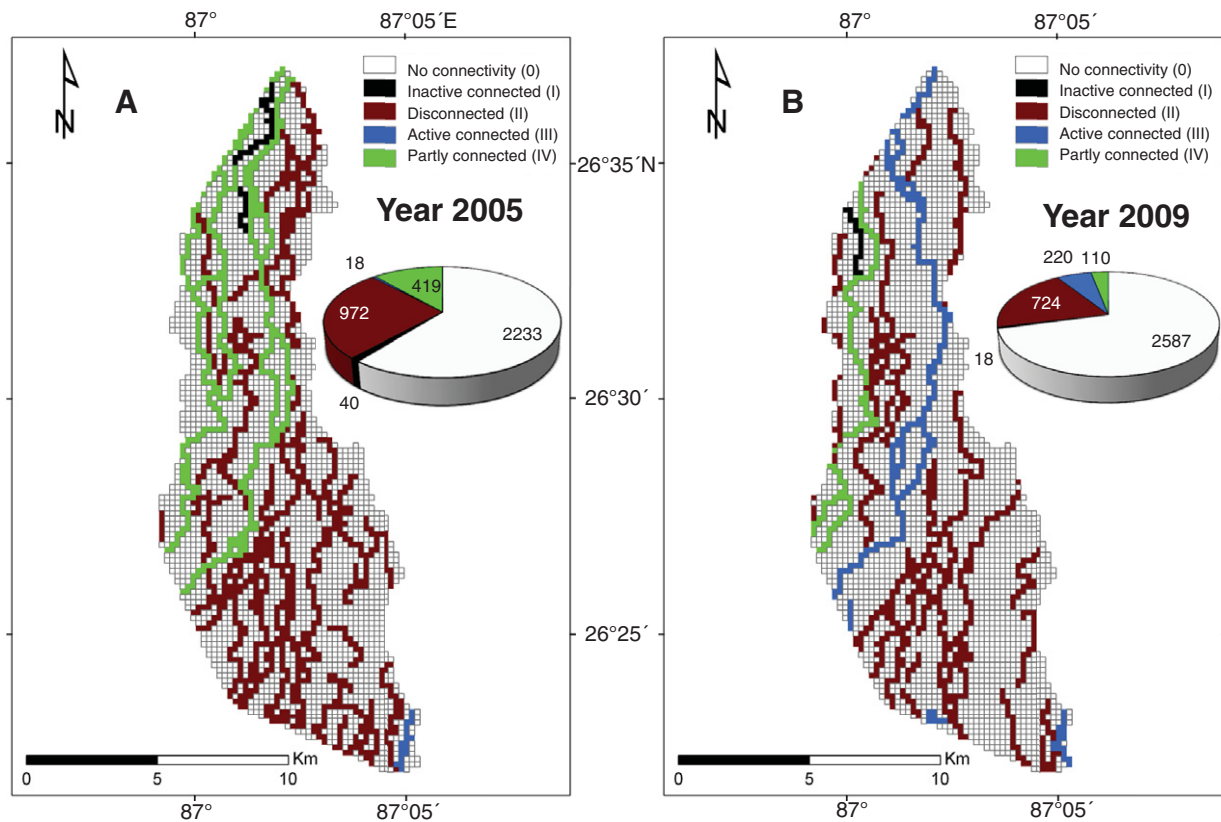


Figure 4. Grid representation of change detection analysis for connectivity structure between 2005 and 2009. Inset pie charts show numbers of links in each class for 2005 and 2009.

Fig. DR3B). A large part of class I has changed to class III, suggesting local wetting of dry channels.

Figure 5A shows the pathway of the predicted avulsive channel (thick red line connected via yellow nodes) using the algorithm described above. The post-avulsion channel on 29 September 2009 (in blue) is also shown. The modeled path matches quite closely with the post-avulsion channel of 2009 in the upper reaches, but shows some deviation in the lower reaches where the modeled path intersects anthropogenic structures. We also tested the accuracy of our prediction by creating a buffer of 500 m on each side of the avulsion channel and computing the percentage of length of the modeled channel within the buffer zone. As a first approximation, this analysis generally validates the model and we obtained an accuracy of ~74%, which is reasonable given the moderate vertical resolution of the SRTM data and the uncertainty introduced by anthropogenic interventions. We therefore conclude that this approach can be used to predict the path of an avulsion channel from any likely future breach point in the embankment. Our analysis supports the experimental results of Jerolmack and Paola

(2007, p. 269), who concluded that the paleochannel network plays an important role for "steering flood flows and serving as avulsion pathways."

Figure 5A also shows the connectivity indices (I_c and $C\%$) for the avulsion belt for the Kusaha breach for 2005 and 2009. The high I_c value (1.66) and low $C\%$ (37.55) for the year 2005 imply a low degree of connectivity, and both indices for 2009 (I_c decreases to 0.535 and $C\%$ increases to 65.13) reflect a significant improvement in the connectivity structure following the August 2008 breach and avulsion. These observations match well with the change detection analysis discussed here (Fig. 4), which also showed that the number of active connected links (class III) increased significantly after the 2008 avulsion event.

We use this model to examine channel connectivity of a possible breach point upstream of Kusaha that has high vulnerability based on avulsion threshold analysis (R. Sinha, unpublished data) and field observations. The modeled avulsion channels using the distribution of nodes from the 2000 SRTM data and the 2009 Landsat TM satellite image-derived channel network are shown in Figure 5B. From the predicted

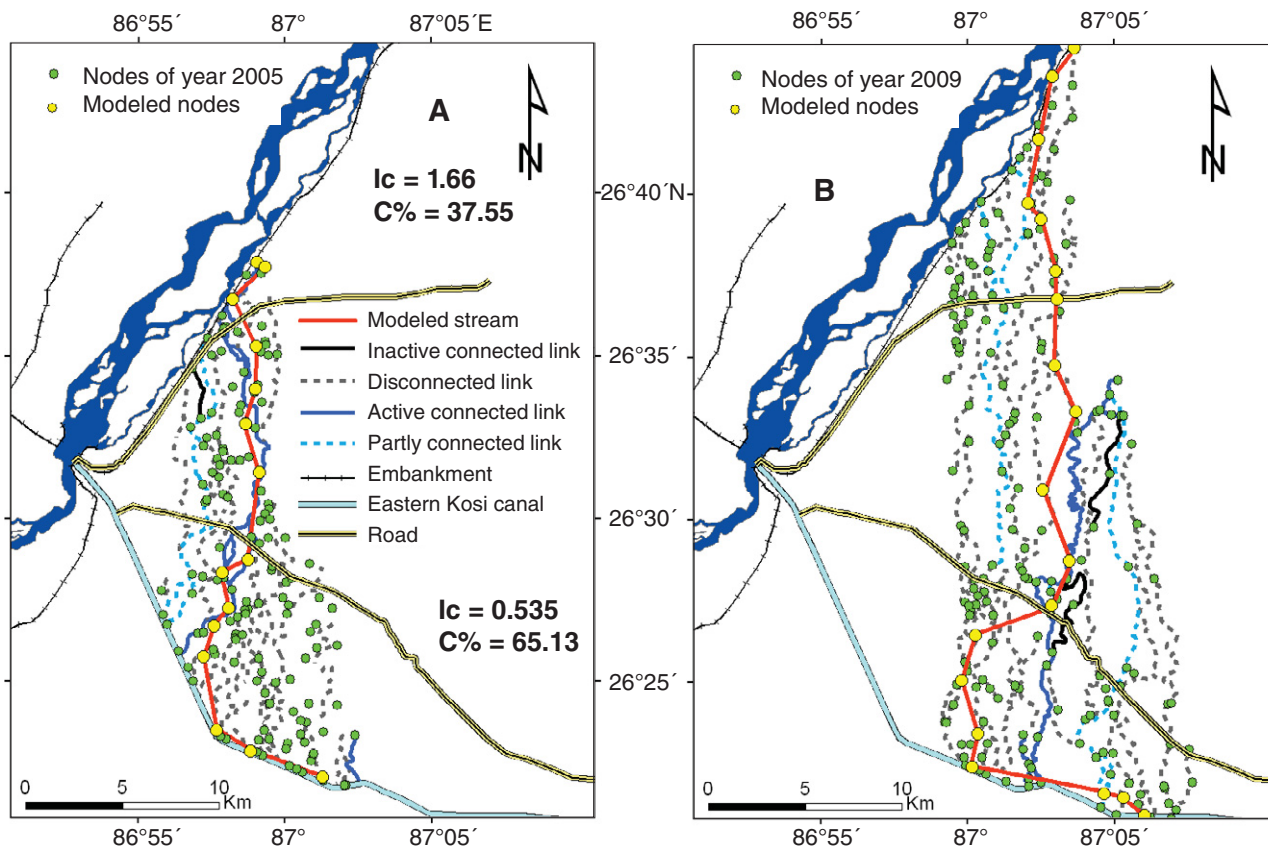


Figure 5. A: Distribution of manually extracted nodes (green dots) from channel network of 2005 used to predict pathway during 2008 avulsion event (yellow dots joining red line), using algorithm based on topography and distance criteria; post-avulsion channel as of 29 September 2009 (blue line) is also plotted. High connectivity index, I_c (1.66) and low percentage connectivity, $C\%$ (37.55) for 2005 imply low degree of connectivity. Decrease in I_c to 0.535 and increase in $C\%$ to 65.13 reflect significant improvement in connectivity structure following August 2008 breach and avulsion. **B:** Modeled pathway of avulsion channel from upstream point with high vulnerability to breaching using nodes derived from channel network of 2009. Blue line represents active channel.

channel network in such a postulated avulsion belt, a first approximation of the inundation zone can also be made by estimating the width of the avulsion channel belt. The width of the Kusaha avulsion belt and that of the modeled upstream vulnerable zone are similar (Fig. 5B).

CONCLUSIONS

The 2000 SRTM data in conjunction with the channel connectivity structure of 2005 show that there is a good match (~74%) between the modeled and observed avulsion channels formed during the August 2008 Kosi avulsion following a breach in its eastern embankment. The change detection analysis of the connectivity structure reflects an increase in the structural connectivity between 2005 and 2009. The connectivity indices also show a significant change during this period, suggesting an improvement in connectivity structure following the August 2008 avulsion. The model has also been used to postulate the possible pathway of an avulsion channel from a similar vulnerable point upstream of Kusaha. These analyses have the potential to be used in flood risk assessment.

ACKNOWLEDGMENTS

We thank the Ministry of Earth Sciences, New Delhi, for providing the financial assistance for this research through a generous grant (MOES/16/01/09/09-RDEAS) to Sinha.

REFERENCES CITED

Bracken, L.J., and Croke, J.C., 2007, The concept of hydrological connectivity and its contribution to understanding runoff-dominated geomorphic systems: *Hydrological Processes*, v. 21, p. 1749–1763, doi:10.1002/hyp.6313.
Chakraborty, T., Kar, R., Ghosh, P., and Basu, S., 2010, Kosi megafan: Historical records, geomorphology and the recent avulsion of the Kosi

River: *Quaternary International*, v. 227, p. 143–160, doi:10.1016/j.quaint.2009.12.002.
Desai, C.G., 1982, *The Kosi River: Its morphology and mechanics in retrospect and prospect*: New Delhi, Central Water Commission, Ministry of Irrigation, Government of India, 90 p.
Gole, C.V., and Chitale, S.V., 1966, Inland delta building activity of Kosi River: *American Society of Civil Engineers Journal of the Hydraulics Division*, v. 92, p. 111–126.
Jain, V., and Tandon, S.K., 2010, Conceptual assessment of (dis)connectivity and its application to the Ganga River dispersal system: *Geomorphology*, v. 118, p. 349–358, doi:10.1016/j.geomorph.2010.02.002.
Jerolmack, D.J., and Paola, C., 2007, Complexity in a cellular model of river avulsion: *Geomorphology*, v. 91, p. 259–270, doi:10.1016/j.geomorph.2007.04.022.
McFeeters, S.K., 1996, The use of normalized difference water index (NDWI) in the delineation of open water features: *International Journal of Remote Sensing*, v. 17, p. 1425–1432, doi:10.1080/01431169608948714.
Mishra, D.K., 2008, The Kosi and the embankment story: *Economic and Political Weekly*, v. 43, p. 47–52.
Sinha, R., 2009, The great avulsion of Kosi on 18 August 2008: *Current Science*, v. 97, p. 429–432.
United Nations Institute for Training and Research, 2008, *Flood waters in Sunsari & Saptari districts, Nepal*: United Nations Institute for Training and Research (UNITAR) Operational Satellite Applications Programme (UNOSAT), scale 1:180,000.
Wainwright, J., Turnbull, L., Ibrahim, T.G., Artza, I.L., Thornton, S.F., and Brazier, R.E., 2011, Linking environmental regimes, space and time: Interpretations of structural and functional connectivity: *Geomorphology*, v. 126, p. 387–404, doi:10.1016/j.geomorph.2010.07.027.

Manuscript received 4 March 2013
Revised manuscript received 11 June 2013
Manuscript accepted 18 June 2013

Printed in USA